Int. J. Electrochem. Sci., 8 **(2013)** 12387 - 12401

International Journal of
ELECTROCHEMICAL
SCIENCE
www.electrochemsci.org

Synthesis and Electrochemical Studies of Some Metal Complexes with Phosphorus Schiff Base Ligand

Salwa A.H. Elbohy

Department of Chemistry, Faculty of Science (Girls), Al Azhar University, Nasr City, Cairo, Egypt
E-mail: salwaalbohy@yahoo.com

Received: 29 May 2013 / *Accepted:* 12 August 2013 / *Published:* 20 October 2013

The complexes of type [CrLCl]0.5H_2O and [ML(H_2O)]nH_2O in which M = Co(II); n = 4.5, Ni(II); n = 4.5, Cu(II); n = 7 and Zn(II); n = 6.5 ions and L is N,N'-bis(2–Hydroxybenzylidene)–1,1–diaminomethylphosphine-oxide, were prepared and their structures characterized by elemental analysis, IR, ^{1}H NMR, ^{31}P NMR, XRD, GA, CV, mass, molar conductance, magnetic moment and UV–Visible spectra. Antimicrobial activities have been studied using the agar-disc diffusion technique, and the higher antimicrobial activity has been observed for the chromium(III) complex compared to the other metal complexes. The redox behavior of complexes was investigated by cyclic voltammetry.

Keywords: Synthesis; ^{31}P NMR; Spectroscopic; antimicrobial activity

1. INTRODUCTION

In recent years, the structural feature of four-memberedN$_2$P$_2$ ring compounds in which the coordination number of P varies from three to five have attached considerable attention [1,2]. Heterocycles with P–C, P–N, P–O, and P–S bonds, in addition to their great biochemical and commercial importance [3,4], play a major role in some substitution mechanisms heterocycles had been found to be potentially carcinostatics [3] among other pharmacological activities. The introduction of tervalent P centers in the ring enhanced the versatility of the heterocycles in complexing with both hard and soft metals. Since the tervalent P centers could stabilize transition metals in low oxidation states [3,4], such complexes could be potential homogeneous or phase-transfer catalysts in various organic transformations [3]. There is considerable current interest in compounds containing spiro and ansaorganic P rings [5]. The present-work aims chiefly to prepare the metal complexes of N,N'-bis(2-Hydroxybenzylidene)-1,1-diaminome-thylphosphineoxide (H_2L). In this

work, novel N,N'-bis(2-Hydroxybenzylidene)-1,1-diaminodiaminome-thylphosphineoxide (H_2L) was prepared and its behavior towards some transition metal ions was studied using different techniques such as elemental analyses, IR, ^{1}H NMR, EPR, solid reflectance, molar conductance, magnetic moment, mass spectra, UV-Vis, and TGA. Also, the antibactericidal and antifungicidal activities of these compounds against some pathogens were studied. The proposed structure for H_2L is shown in Scheme 1.

2. SYNTHESIS

2.1. Synthesis of ligand (H_2L)

To a magnetically stirred solution of phosphoryltrichloride (0. 1 mol, 15.0 g) in dry 1,4-dioxane (10 ml) was added drop-wise of N,N'-bis(2-Hydroxybenzylidene)-1,1-diaminomethane (0.1 mol, 25.5 g) in dry 1,4-dioxane (10 ml) in the presence of the Et_3N (1 ml) as a base in in dry 1,4-dioxane (3 ml) over 20 min. The mixture was stirred for 7 h at room temperature. After the completion of the reaction (HCl gas ceased to evolve), the solvent was removed under reduced pressure and the viscous residue was purified by flash column chromatography (silica gel; petroleum ether-ethyl acetate [10: 2]). The solvent was removed under reduced pressure and the product H_2L was obtained. The product obtained give elemental analyses (Table 1) consistent with the proposed structure.

2.2. Synthesis of metal complexes

The metal complexes were prepared by adding dropwise a hot aqueous (ca. 60°C) solution (100 mL) of the metal chlorides (0.1 mol) to a solution of H_2L (0.1 mol) in tetrahydrofuran (100 mL) while stirring continuously. After complete addition of the metal salt solution, the reaction mixture was heated under reflux for about 3 hours under dry conditions. The complexes obtained were filtered, washed with water, ethanol, and tetrahyrofuran and then dried in vacuo. The complexes are partially soluble in dioxan, CH_3CH_2OH, CH_3OH, $CHCl_3$, DMF, MeCN and insoluble in nonpolar solvents. The products obtained give elemental analyses (Table 1) consistent with the proposed structures.

3. EXPERIMENTAL

All chemicals used in this investigation were of analar grade, provided by B.D.H. chemicals. These include $CrCl_3{\cdot}6H_2O$, $CoCl_2{\cdot}6H_2O$, $NiCl_2{\cdot}6H_2O$, $CuCl_2{\cdot}2H_2O$, and $ZnCl_2$ methyl amine, 2-aminothiophene and phosphorus pentachloride. The solvents used were dry ethanol, dioxane, dry diethylether, MeCN, dimethylformamide (DMF) and deutrated dimethylsulfoxide (DMSO). N,N'-bis(2-Hydroxybenzylidene)-1,1-diaminomethane have been prepared and purified using the method previously[6]. The C, H, and N data were obtained by using a Carlo-Erba 1106 elemental analyzer. The P content was determined gravimetrically as phosphoammonium molybdate using the Voy method

[7]. Metal contents were determined complexometrically by standard EDTA titration. The infrared spectra were recorded on a Shimadzu FT-IR spectrometer using KBr discs. Molar conductances of the phosphine Schiff base ligands and their transition metal complexes were determined in DMSO (~10^{-3} M) at room temperature using a Jenway Model 4070 conductivity meter. ^{1}H and ^{13}C NMR spectra were taken on a Varian Mercury 300MHz Em-360-60 MHz instrument. TMS was used as internal standard and $CHCl_3$ as solvent. ^{31}P NMR spectra were run, relative to external H_3PO_4 (85%), with a varian FT-80 spectrometer at 365MHz. The solid reflectance spectra were measured using a Shimadzu PC3101 UV-VIS-NIR scanning spectrophotometer. Magnetic measurements were recorded by the Gouy method at room temperature using a magnetic susceptibility balance (Johanson Mathey), Alfa product, Model No. (MK). The TGA were recorded on a Shimadzu TGA-50H. TGA was carried out in a dynamic nitrogen atmosphere (20 mL min^{-1}) with a heating rate of 10°C min^{-1}. The ultraviolet spectra were recorded on a Perkin-Elmer Lambda–3B UV-VIS spectrophotometer. The mass spectra were performed using a Shimadzu-Ge-Ms-Qp 100 EX mass spectrometer using the direct inlet system. EPR spectra of Cr(III) and Cu(II) the complexes were recorded as polycrystalline samples, at room temperature, on an E4-EPR spectrometer using the DPPH as the g-marker. The biological activity experiments were carried out at the Microbiology Laboratory at Bab-Al-Sheria University Hospital, Al-Azhar University. Electrochemical measurements were carried out in Electrochemical Analyser model BAS-50 voltammograph. The three-electrode cell contained a reference Ag/AgCl electrode, Pt wire auxillary electrode and glassy carbon.

4. CHEMISTRY

4.1. Synthesis of ligand (H_2L) and, their metal complexes (1-5).

Table 1. Elemental analyses, melting points, colours, yields and composition of ligand (H_2L) and its corresponding metal complexes

Compd. No. M.F. (M.Wt)	[M.p.] (°C)	Color	Yield(%)	Elemental analyses Found (Calc.), %				
				M	C	H	N	P
$C_{15}H_{13}N_2O_3P$(300) H_2L	101	Yellow	96	-	60.04 (60.00)	4.34 (4.36)	9.35 (9.33)	10.30 (10.32)
(1) $C_{15}H_{12}ClCrN_2O_{3.5}P$(395) $[CrLCl]0.5H_2O$	>300	Olive green	94.3	13.18 (13.17)	45.66 (45.65)	3.03 (3.06)	7.13 (7.10)	7.84 (7.85)
(2) $C_{15}H_{22}CoN_2O_{8.5}P$(456) $[CoL(H_2O)]4.5H_2O$	>300	Violet	92.6	12.95 (12.92)	39.47 (39.49)	4.86 (4.86)	6.14 (6.14)	6.80 (6.79)
(3) $C_{15}H_{22}N_2NiO_{8.5}P$(456) $[NiL(H_2O)]4.5H_2O$	>300	Green	92.7	12.84 (12.87)	39.58 (39.51)	4.86 (4.86)	6.16 (6.14)	6.79 (6.79)
(4) $C_{15}H_{27}CuN_2O_{11}P$(506) $[CuL(H_2O)]7H_2O$	>300	Royal blue	97.8	12.55 (12.56)	35.61 (35.61)	5.37 (5.38)	5.55 (5.54)	6.11 (6.12)
(5) $C_{15}H_{26}N_2O_{10.5}PZn$(499) $[ZnL(H_2O)]6.5H_2O$	>300	Light yellow	93.2	13.17 (13.11)	36.12 (36.12)	5.24 (5.25)	5.63 (5.62)	6.20 (6.21)

Phosphorus Schiff base (H_2L) was prepared by the reaction of phosphoryltrichloride with the respective Schiff base to obtain the desired Schiff base as shown in Scheme 1. This was only soluble in methyl alcohol, ethyl alcohol, dioxane, DMF and DMSO. The composition of which is consistent with

their micro-analytical and spectral data. 2. The metal complexes (1-5) were prepared in a molar ratio [metal: ligand (1:1)]. Chromium, cobalt, copper, nickel and zinc metals were used as chloride salts. Physical measurements and analytical data of the complexes (1-5) are given in (Table 1)

5. PHARMACOLOGY

5.1. Antibacterial and antifungal activities

The screening data obtained for the compounds under study against the sensitive organisms *S. aureus, S. pyogenes, P. fluorescens, P. phasiolicola, A. alternate, F. oxysporum, A. fumigatus, and C. albicans* using the disc-agar diffusion technique [5,8] are summarized in Table 2. A comparison of all tested compounds towards the different organisms brings out the following fats to light:

• The highest antimicrobial activity among the group of the tested compounds was observed against the fungi strains.

• The phosphorus Schiff base ligand (H_2L) displayed intermediate activity against all types of bacteria and fungi species.

• Generally the activity of the free ligand was increased upon complexation with metal ions; the enhancement in activity can be explained on the basis of chelation theory [5,7,9]. Chelation reduces the polarity of the metal ion considerably, mainly because of the partial sharing of its positive charge with donor groups and the possible p electron delocalization over the whole chelate ring. Chelation not only reduces the polarity of metal ion, but also increases the lipophilic character of the chelate. As a result of this, the interaction between the metal ion and the cell walls s favored, resulting in interference with normal cell processes.

• There are other factors which also increases the activity are solubility, conductivity and bond length between the metal and ligand.

• It was also noted that the toxicity of the metal chelates increases on increasing the metal ion concentration.

• The bounded metal may block enzymatic activity of the cell or else it may catalyze toxic reactions among cellular constituents.

• The effect of all metal complexes towards the fungi species was greater than the bacteria species.

• The metal complexes (2–5) displayed intermediate activity against all types of bacteria and fungi species with inhibition zone values greater than the free ligand (H_2L).

• Cr(III) complex (1) had a higher degree of activity than all the other metal complexes or the free ligand (H_2L) against all types of bacteria and fungi It displayed high activity. Only Cr(III) complex (1) had an effect comparable with that of the standards (Chloramphenicol, Cephalothin, and Cycloheximide) towards the tested organism. This may have been due to the trivalent state of the metal ion and/or the increase in the number of chloride around the metal ion [5,7].

Table 2. Antimicrobial screening results of the compounds under study.

Compd. No.	Gram-positive bacteria		Gram-negative bacteria		Fungi			
	Staphylococcus aureus	Streptococcus pyogenes	Pseudomonas phaseolicola	Pseudomonas fluorescens	Alternarie alternate	Fusarium oxysporum	Aspergillus fumigatus	Candida albicans
(H_2L)	(35) 13	(37) 14	(36) 15	(40) 14	(43) 15	(48) 16	(47) 18	(49) 17
1	(39) 16	(39) 18	(54) 19	(43) 18	(63) 18	(62) 22	(57) 23	(66) 25
2	(37) 13	(38) 15	(50) 16	(43) 15	(62) 15	(60) 20	(60) 23	(67) 24
3	(38) 15	(37) 16	(57) 19	(52) 19	(62) 14	(63) 21	(53) 20	(64) 23
4	(35) 14	(38) 16	(54) 18	(57) 17	(63) 15	(61) 21	(61) 23	(**62**) 24
5	(37) 16	(66) 25	(88) 31	(79) 28	(83) 16	(76) 34	(77) 37	(**86**) 35
$CrCl_3.6H_2O$	(26) 10	(26) 10	(35) 12	(30) 11	(45) 17	(46) 16	(35) 14	(36) 13
$CoCl_2.6H_2O$	(49) 19	(49) 19	(44) 15	(27) 10	(43) 17	(46) 16	(40) 16	(50) 18
$NiCl_2.6H_2O$	(36) 14	(36) 14	(53) 18	(35) 13	(33) 14	(37) 13	(45) 18	(31) 11
$CuCl_2.6H_2O$	(46) 18	(46) 18	(50) 17	(38) 14	(41) 13	(43) 15	(35) 14	(33) 12
$ZnCl_2$	(51) 20	(51) 20	(59) 20	(57) 21	(52) 18	(57) 20	(49) 19	(61) 22
R.S.	(100) 39	(100) 38	(100) 34	(100) 37	(100) 35	(100) 35	(100) 40	(100) 36

• The test was done using the agar-disc diffusion method.

• % Activity index in partnesses.

• R. S., Reference standard: Chloramphencol, Cephalothin, and Cycloheximide were used as standard reference for Gram-positive bacteria, Gram-negative bacteria, andantifungal, respectively.

• Inhibition values: 3–13 low activity; 14–24 intermediate activity; 25–32 high activity; and >32 very high activity.

6. RESULTS AND DISCUSSION

6.1. Spectroscopic characterization of compounds

6.1.1. The ligand (H_2L)

The analytically pure ligand H_2L was readily synthesized with very good yield (96%) by phosphorus Schiff base reaction of N,N'-bis(2-Hydroxybenzylidene)-1,1-diaminomethane with one equivalent of phosphoryltrichloride in the presence of a base at room temperature. The ligand may show keto-enol tautomerism because it contains the amide bonds. The IR spectrum Table 3 does not show a ν(OH) band at 3550 cm^{-1} but shows the bands at 3270 and 3197 cm^{-1} corresponding to ν_{as}(NH) and ν_s(NH), indicating that in solid state, the ligand exists in the keto form[7, 10], The ν(P−C) stretching vibration is observed at 1430 cm^{-1} [11]. However, the ^{1}H NMR spectrum Table 4 of ligand exhibits a sharp singlet at 11.76 ppm due to enolic –OH which indicates that the amide groups are transformed into iminol groups in solution.

The ^{31}P–NMR of the ligand records a signal at δ = 61.03 ppm, which supports the phosphorus carbide (P–C) group [12].

The electronic spectrum of H_2L Table 5 in ethanol showed absorption bands at 245–395 nm regions which is due to intraligand π→π* and n→π* transitions involving molecular orbital of the thiophene ring, a broad shoulder at approximately 434 nm were observed. The latter band is attributed

to a n(oxygen) →π* transition of the dipolar zwitterionic structure or keto-amine tautomer of H_2L [13]. The electron impact mass spectrum Table 6 of the free ligand, confirms the proposed formula by showing a peak at 299 u corresponding to the ligand moiety [($C_{15}H_{13}N_2O_3P$) atomic mass 300u]. The series of peaks in the range, i.e. 64, 110 and 165 u, etc., may be assigned to various fragments and their intensity gives an idea of stability of fragments.

Table 3. Characteristic IR bands of the ligand and its metal complexes.

assignments	Ligand (H_2L)	1	2	3	4	5
$\nu(NH)_{asym.}$	3270br	–	–	–	–	–
$\nu(NH)_{sym.}$	3197br	–	–	–	–	–
ν(P– C)	1430m	1321m	1322m	1323m	1320m	1321m
Amide I	1688m	1665m	1664m	1665m	1664m	1662m
Amide II	1567m	1579m	1579m	1586m	1587m	1583m
ν(C–N)	1358m	1333m	1333m	1329m	1228m	1328m
$\nu(C–H)_{aromatic}$	3033m	3030m	3034m	3030m	3033m	3033m
$\nu(C–H)_{aliphatic}$	2924s, 2856m	2924s, 2856m	2924s, 2856m	2924s, 2856m	2924s, 2856m	2924s, 2856m
$\rho r(H_2O)$	-	788m	830m	845s	745s	798s
$\rho w(H_2O)$	-	635m	615m	615s	627s	635s
ν(C=C)phenyl	1368m	1363m	1336m	1336 s	1336m	1336 s
ν(C–C)	1254m	1255m	1255m	1255m	1254m	1254m
δ(O–M−O)	-	208 w	209 w	208 w	208 w	208 w
δ(O–M–N)	-	216w	218w	216 w	217 w	218 w
δ(O–M−P)	-	233 w	233 w	228 w	228 w	227 w
δ(N–M–P)	-	224v.w	228 v.w	224 v.w	217 v.w	222 v.w
ν(M–N)	-	275m	270m	278m	292m	293m
ν(M–O)	-	333m	328m	333m	338m	340m
ν(M–P)	-	518m	470m	560m	523m	547m

Where br = broad, s = strong, m = medium, w = weak, v.w = very weak

Table 4 .The ^1H, ^{13}C and ^{31}P NMR chemical shifts (ppm) for the phosphine Schiff base, H_2L, ligand and its Zn(II) complex in $CDCl_3$ solvent**.**

Compound	^1H NMR		^{13}C NMR		^{31}P NMR	
	Chemical shift, δ(ppm)	Assignment	Chemical shifts (δ, ppm)	Assignment	Chemical shifts (δ, ppm)	Assignment
H_2L	11.76*	s, 2H, –OH	164.34	δ(C=O)	61.03	δ(C–P)
	8.12*	m, 2H, –NH	112.42-152.45	δ(C–N)		
	8.32*	br, 2H, CH=N–	116.15-157.26	δ(C-arom.)		
	7.8-6.9	Phenyl ring protons	32.24	δ(C–H)		
	2.42	s, –CH	22.34	δ(C–P)		
$[ZnL(H_2O)]6.5H_2O$	–	2H, –OH	162.23	δ(C=O)	57.05	δ(C–P)
	–	m, 2H, –NH	108.12-150.53	δ(C–N)		
	8.32	br, 2H, CH=N–	116.54-156.00	δ(C-arom.)		
	7.8-6.9	Phenyl ring protons	32.24	δ(C–H)		
	2.43	s, –CH	20.23	δ(C–P)		
	3.32	s, 8H, coordinated H_2O protons				

(1) s: singlet, br: broad, m: multiplet.

(2) Data given from the spectra depicted in Scheme 1.

(3) ^{1}H and ^{13}C chemical Shifts were recorded in $CDCl_3$ solvent and referenced internally with respect to TMS.

(4) ^{31}P chemical shifts were recorded in $CDCl_3$ and referenced externally with respect to H_3PO_4 (85%).

(5) Asterisks (*) denote the bands disappeared after the addition of D_2O.

6.2. Complexes

On the basis of elemental analysis data Table 1, all the complexes have the general composition $[CrLCl]0.5H_2O$ and $[ML(H_2O)]nH_2O$, where M= Co(II); n = 4.5, Ni(II); n = 4.5, Cu(II); n = 7, and Zn(II); n = 6.5, L = N,N'-bis(2-Hydroxybenzylidene)-1,1-diaminomethylphosphine-oxide. The complexes were obtained in powder form. These were found to be sufficiently soluble in chloroform and DMSO for spectral measurements. Various attempts to obtain the single crystals of the complexes have so far been unsuccessful.

6.2.1. Molar conductance

The molar conductance values in DMSO at 25 °C Table 5 for the complexes were found to be in the range 9.64–13.84 Ω^{-1} mol^{-1} cm^2. The relatively low values indicate the non-electrolytic nature of these complexes [5]. This can be accounted for by the satisfaction of the bi- or tri-valency of the metal by the chloride. This implies the coordination of the anions to the metal ion centers.

Table 5. Molar conductance, magnetic moment and electronic spectral data of the complexes.

Complex	Molar conductance ($\Omega^{-1}cm^2mol^{-1}$)	Geometry	μ_{eff} (B.M.)	Band assignments	λmax (cm^{-1})
$[CrLCl]0.5H_2O$	12.32	Octahedral	3.87	$^4B_1g \rightarrow {}^4Eag(\nu_1)$ $^4B_1g \rightarrow {}^4B_2g(\nu_2)$ $^4B_1g \rightarrow {}^4Ebg(\nu_3)$ $^4B_1g \rightarrow {}^4A_1g(\nu_4)$	16,945 24,560 27,476 38,469
$[CoL(H_2O)]4.5H_2O$	9.64	Octahedral	3.88	$^4T_1g \rightarrow {}^4T_2g(F)(\nu_1)$ $^4T_1g \rightarrow {}^4A_2g(F)(\nu_2)$ $^4T_1g \rightarrow {}^4T_1g(P)(\nu_3)$	13,653 15,155 25,007
$[NiL(H_2O)]4.5H_2O$	11.72	Octahedral	2.74	$^3A_2g(F) \rightarrow {}^3T_2g(F)(\nu_1)$ $^3A_2g(F) \rightarrow {}^3T_1g(F)(\nu_2)$ $^3A_2g(F) \rightarrow {}^3T_1g(P)(\nu_3)$	14,372 15,794 21,456
$[CuL(H_2O)]7H_2O$	12.55	Octahedral	2.13	$Eg \rightarrow {}^3T_2g$ (G)	17,357
$[ZnL(H_2O)]$ $6.5H_2O$	13.84	Octahedral	diamagnetic	LMCT(M←N)	25,687

6.2.2. IR spectra and mode of bonding

The assignments of the main IR absorption bands of the ligand and its complexes are given in Table 3. The free ligand displays the IR bands at 3270 and 3197cm^{-1} corresponding to the ν_{asym}(NH)

and ν_{sym}(NH) stretching vibrations, respectively. The spectrum exhibits the IR bands at 1430, 1688 and 1567 cm^{-1} which may be assigned to the phosphorus carbide [P–C], amide I [ν(C=O)] and amide II [ν(C=N) +δ(NH)] stretching vibrations. On complex formation, the position of P–C and amide I are shifted to the lower wave numbers [7, 10] while the amide II band shows the positive shift. This indicates that the amide oxygen, P–C phosphorus and azomethine nitrogen atoms are coordinated to the metal ion. This coordination behaviour of the ligand is also proved by the appearance of IR bands due to ν(M–N), ν (M–O) and ν(M–P) vibrations in the range 270–293, 328–340 and 470–560cm^{-1}, respectively [5].

The chloro complex (1) shows the band at 332 cm^{-1} due to ν(M–Cl) [7]. The complexes (1–5) also display bands due to coordinated water molecules [7]. The bands in the range 745–830 cm^{-1} and 615–635 cm^{-1} appeared in the spectra of these complexes which may be assigned to ρr(H_2O) and ρw(H_2O) [7]. Also, The band at 1376–1378 cm^{-1} in all the complexes is due to the ν(CH) frequency, is not affected upon complexation. Furthermore, the aliphatic protons are not greatly affected upon complexation [7].

6.2.3. Mass spectra

Table 6. Important mass peaks for the complexes (1-5) studied

Complex no.	Mass assignments	M	m/z
1	$[C_{15}H_7CrNOP]^+$	300	300
	$[C_8H_{10}CrP]^+$	189	189
	$[C_6H_3NOP]^+$	136	136
	$[C_4H_3]^+$	51	51
2	$[C_{10}H_{14}CoNO_4P]^+$	*302*	*302*
	$[C_4H_{11}CoOP]^+$	*165*	*165*
	$[C_4H_3Co]^+$	*110*	*110*
	$[C_5H_5]^+$	*65*	*65*
3	$[C_{10}H_{17}NNiO_5P]^+$	*320*	*320*
	$[C_4H_{11}NiOP]^+$	*165*	*165*
	$[C_4H_8Ni]^+$	*115*	*115*
	$[C_5H_5]^+$	*65*	*65*
4	$[C_{12}H_{16}CuNO_6P]^+$	*365*	*365*
	$[C_9H_{11}CuNO_4P]^+$	*292*	*292*
	$[C_7H_{10}CuNO_3P]^+$	*251*	*251*
	$[C_6H_7CuOP]^+$	*190*	*190*
	$[C_3H_4CuP]^+$	*135*	*135*
	$[C_5H_3]^+$	*63*	*63*
5	$[C_{10}H_{25}NO_4PZn]^+$	*320*	*320*
	$[C_7H_{20}NO_3PZn]^+$	*263*	*263*
	$[C_6H_{12}Zn]^+$	*150*	*150*
	$[C_4H_3]^+$	*51*	*51*

The fragmentation patterns of the studied complexes obtained from the mass spectra are given in Table 6. The FAB mass spectra of Cr(III), Co(II), Ni(II), Cu(II), and Zn(II), phosphine complexes have been recorded. All the spectra exhibit parent peaks due to molecular ions (M^+). The proposed molecular formula of theses complexes was confirmed by comparing their molecular formula weights

with m/z values. The molecular ion (M^+) peaks obtained for various complexes are as follows: (1) m/z = 396(Chromium(III)complex), (2) m/z = 456(Cobalt(II)complex), (3) m/z = 454(Nickel(II)complex) (4) m/z = 503 (Copper(II) complex) (5) m/z = 501 (Zinc(II)complex). This data is in good agreement with the proposed molecular formula for these complexes i.e. [CrLCl]0.5H_2O and [ML(H_2O)]nH_2O, where M= Co(II); n = 4.5, Ni(II); n = 4.5, Cu(II); n = 7, and Zn(II); n = 6.5, L = N,N'-bis(2-Hydroxybenzylidene)-1,1-diaminomethylphosphineoxide. This confirms the formation of the phosphine frame. In addition to the peaks due to the molecular ions, the spectra exhibit peaks assignable to various fragments arising from the thermal cleavage of the complexes. The peak intensity gives an idea of the stability of the fragments.

6.2.4. Electronic and EPR spectra measurements

The electronic spectra of the complexes are presented in Table 5. The visible spectrum of chromium complex, shows four absorption bands at 16,945, 24,560, 27,476, and 38,469 cm^{-1} assignable to $^4B_1g \rightarrow {}^4E^ag(\nu_1)$, $^4B_1g \rightarrow {}^4B_2g(\nu_2)$, $^4B_1g \rightarrow {}^4E^bg(\nu_3)$ and $^4B_1g \rightarrow {}^4A_1g(\nu_4)$ transitions respectively, which indicates the possibility of octahedral geometry of the metal complex [5,14-15]. The EPR spectrum was recorded as polycrystalline sample at room temperature and the *g*-value was calculated by using the expression: $g = 2.0023(1-4\lambda/10Dq)$, where λ is the orbit spin coupling constant for the metal ion in the complex. The calculated *g*-value is 1.98 [14].

The electronic spectrum of the Co(II) complex displays three bands at 13,653, 15,155 and 25,007 cm^{-1} . These bands may be assigned to following transitions $^4T_1g \rightarrow {}^4T_2g(F)$ (ν_1), $^4A_2g \rightarrow {}^4T_1g(F)$ (ν_2) and $^4A_2g \rightarrow {}^4T_1g(P)$ (ν_3), respectively. The position of bands suggest octahedral geometry of Co(II) complex [14,16]. EPR spectrum of complex under study was recorded at liquid nitrogen temperature as polycrystalline sample. A broad signal was obtained, because the rapid spin lattice relaxation of Co(II) broadened the lines at higher temperature. The large deviation of the *g* values ($g_\parallel$ = 2.527 and $g\perp$ = 2.958) from the spin only value (g = 2.0023) is due to large angular momentum contribution [14].

Electronic spectrum displays bands at 14,362, 15,794 and 21,456 cm^{-1} These bands may be assigned to $^3A_2g \rightarrow {}^3T_2g(F)(\nu_1)$, $^3T_1g(F) \rightarrow {}^3A_2g$ (ν_2) and $^3T_1g(F) \rightarrow {}^3T_1g$ (ν_3) transitions, respectively. It suggests octahedral geometry of Ni(II) complex [14,15].

The electronic spectrum of the Cu(II) complex gave a band at 17,357cm^{-1}, suggesting the existence of a transition from d_{xy}, d^2_z and d_{xz}, d_{yz} transfer to the antibonding and half-filled dx^2-sy^2 level which is consistent with an octahedral configuration.

EPR spectrum of Cu(II) complex was recorded at room temperature as polycrystalline samples and in DMF solution, on the *x*-band at 9.1 GHz under the magnetic field strength 3400 G. Polycrystalline spectrum shows a well-resolved anisotropic broad signal. The analysis of spectra give $g_\parallel$ = 2.19 and $g\perp$ = 2.11. The trend $g_\parallel > g\perp > 2.0023$, observed for the complex, under study, indicates that the unpaired electron is localized in dx^2-y^2 orbital of the Cu(II) ion and the spectral features are characteristic for axial symmetry. Octahedral elongated geometry is thus confirmed for the aforesaid complex [5, 14-20].

The Zn(II) complex (5) is diamagnetic as expected and its geometry is most probably octahedral similar to the Cu(II), Ni(II) and Co(II) complexes of the H_2L ligand.

6.2.5. Ligand field parameters

Various ligand parameters were calculated for the complexes and are listed in Table 7. The value Dq in Co(II) complexes was calculated from transition energy ratio diagram using the ν_3/ν_2 ratio The Nephelauxetic parameter β was calculated by using the relation $\beta = B$(complex)/B(free ion), where B free ion for Cr(III), Co(II), Ni(II), is 918, 960, and 904 cm^{-1}. The β value lies in the range 0.73–0.87. These values indicate that the appreciable covalent character of metal ligand σ bond [14-16,21].

Table 7. Ligand field parameters of the complexes

Complex	Dq (cm^{-1})	B(cm^{-1})	β	LFSE ($kJmol^{-1}$)
[CrLCl]0.5H_2O	1686	795	0.87	214.23
[CoL(H_2O)]4.5H_2O	1179	800	0.73	96.43
[NiL(H_2O)]4.5H_2O	1496	880	0.78	164.82

6.2.6. Magnetic susceptibility measurements

The Magnetic susceptibility measurements of the complexes are presented in Table 5. Chromium(III) complex shows magnetic moments corresponding to three unpaired electrons, i.e. 3.78 B.M., expected for high-spin octahedral chromium(III) complexes [5,14]. The observed magnetic moment value (3.78 B.M.) for cobalt complex was found to be consistent with half spin octahedral geometry for the cobalt (II) complex. The measured values for the nickel (II) complex was found as 2.74 B.M. which also suggest [5,14] an octahedral environment for the nickel complexes. The magnetic moment values for the copper (II) complex was observed as 2.11 B.M. which lie in the range expected for a d^9-system that contains one unpaired electron consistent to an octahedral geometry [5,14] for the copper complexes. The zinc (II) complex was found to be diamagnetic [5].

6.2.7. ^1H, ^{13}C and ^{31}PNMR spectra

The proton NMR spectra of the ligand H_2L and its diamagnetic Zn(II) complex Table 4 were recorded in DMSO-d_6 solution using tetramethylsilane (TMS) as internal standard. The chemical shifts of the different types of protons of the ligand H_2L and its diamagnetic Zn(II) complex are listed in. The OH signal found at 11.76 ppm in the spectrum of the ligand H_2L is completely disappeared in the spectrum of the Zn(II) complex. This indicates the involvement of the OH group in chelation with Zn(II) through displacement of the OH proton. The signal observed at 3.32 ppm with an integration corresponding to eight protons in case of Zn(II) complex is assigned to four water molecules.

The ^{13}C NMR Spectral data Table 4 also support the authenticity of the proposed structures. The considerable shifts in the positions of carbon atoms adjacent to the imine nitrogen [C–N (δ

112.42-152.45)], enolic oxygen [C=O (δ 164.34)], phosphorus carbide [P– C (δ 22.34)], support the proposed coordination in the complexes. Thus the shifts in the position of carbon atoms adjacent to the coordinating atoms clearly indicate the bonding of the imine (C–N) nitrogen, amido (C=O) oxygen and phosphorus carbide (P–C) phosphorus to the cromium, cobalt, nickel, copper, or zinc atom [5].

The phosphorus thirty one NMR spectra of the ligand H_2L and its diamagnetic Zn(II) complex Table 4 were recorded in DMSO-d_6 solution using 85% H_3PO_4 as an external standard. The P–C proton resonance appeared at 61.03 ppm in the ligand H_2L is shifted to 57.05 ppm in the Zn(II) complex suggests that the phosphorus carbide (P–C) phosphorus is involved in coordination with Zn(II) in the complex [5].

6.2.8. Thermal analyses

Thermogravimetric studies (TGA) for the complexes were carried out within a temperature range from room temperature up to 800 °C. TGA results are in a good agreement with the suggested formulae resulted from microanalyses data Table 1. The determined temperature ranges and percent losses in mass of the solid complexes on heating are given in Table 8 which revealed the following findings:

The Cr(III) complex **(1)** of H_2L gives a decomposition pattern as follows; the first stage is one step within the temperature range of 25–175 °C, representing the loss of 0.5 H_2O (hydrated), 1.5O_2 and HCl gases with a found mass loss of 17.30 % at the end of the thermogram, the metal oxide 1/2Cr_2O_3 was the residue 19.23% (calcd. 19.24%), which is in good agreement with the calculated metal content obtained and the results of elemental analyses Table 1.

The Co(II) complex **(2)** of $H_2L$is thermally decomposed in three stages. The first stage corresponds to a mass loss of 17.74% (calcd. 17.76%) within the temperature range 25–125 °C represents the loss of half past four molecules of hydrated water. The second stage corresponds to a mass loss of 11.82.97% (calcd. 11.84%) within the temperature range 125–245 °C represents the loss of one coordinated water, and O_2 gases. The third stage, 245–765 °C with a found mass loss of 54.80% (calcd. 54.82%), is reasonably accounted for the decomposition of the organic part of the complex leaving out CoO as a residue with a found mass loss of 16.32% (calcd. 16.43%).

The Ni(II) complex **(3)** of H_2L is thermally decomposed in three stages. The first stage corresponds to a mass loss of 7.46% (calcd. 7.84%) within the temperature range 35–125°C represents the loss of half past four molecules of hydrated water. The second stage corresponds to a mass loss of 17.33% (calcd. 17.37%) within the temperature range 125–265 °C represents the loss of one coordinated water, 2NH_3 and O_2 gases. The third stage, 265–785 °C with a found mass loss of 19.27 % (calcd. 19.29%), is reasonably accounted for the decomposition of the organic part of the complex leaving out NiO as a residue with a found mass loss of 16.22% (calcd. 16.37%).

The Cu(II) complex **(4)** of $H_2L$is thermally decomposed in three stages. The first stage corresponds to a mass loss of 24.84% (calcd. 24.90%) within the temperature range 30–130°C represents the loss of seven molecules of hydrated water. The second stage corresponds to a mass loss of 16.53% (calcd. 16.60%) within the temperature range 130–255 °C represents the loss of one

coordinated water and $2NH_3$ gas. The third stage, 255–765 °C with a found mass loss of 42.64% (calcd. 42.68%), is reasonably accounted for the decomposition of the organic part of the complex leaving out CuO as a residue with a found mass loss of 15.23% (calcd. 15.39%).

The Zn(II) complex **(5)** of H_2L is thermally decomposed in three stages. The first stage corresponds to a mass loss of 36.12% (calcd. 36.16%) within the temperature range 30–125°C represents the loss of half past six molecules of hydrated water, $2NH_3$ and O_2 gases. The second stage corresponds to a mass loss of 3.57% (calcd. 3.60%) within the temperature range 125–260 °C represents the loss of one coordinated water. The third stage, 260–805 °C with a found mass loss of 43.24% (calcd. 43.26.89%), is reasonably accounted for the decomposition of the organic part of the complex leaving out ZnO as a residue with a found mass loss of 16.29% (calcd. 16.31%).

Table 8. Thermal decomposition data of H_2L complexes

Comp.no.	complex	TG range(°C)	Found (calcd.%)		Assignments
			Mass loss	Total mass loss	
1	[CrLCl]$0.5H_2O$	25-175	17.30(17.37)		•loss of $0.5H_2O$ (hydrated), HCl and 1.5O gases.
		175-1300	63.00(63.09)	80.30(80.46)	•loss of organic part of the complex and formation of 1/2 Cr_2O_3.
2	[CoL(H_2O)]$4.5H_2O$	25-125	17.74(17.76)		•loss of $4.5H_2O$ (hydrated).
		125-245	11.82(11.84)		•loss of H_2O (coordinated), and O_2 gases.
		245-1300	54.80(54.82)	84.36(84.42)	•loss of organic part of the complex and formation of CoO.
3	[NiL(H_2O)]$4.5H_2O$	35-125	17.33(17.37)		•loss of $4.5H_2O$ (hydrated).
		125-175	18.40(18.42)		•loss of H_2O (coordinated), $2NH_3$ and O_2 gases.
		175-1200	47.34(47.36)	83.07(83.14)	•loss of organic part of the complex and formation of NiO.
4	[CuL(H_2O)]$7H_2O$	30-130	24.84(24.90)		•loss of $7H_2O$ (hydrated).
		130-255	16.53(16.60)		•loss of H_2O (coordinated), 2 NH_3 and O_2 gas.
		255-1200	42.64(42.68)	84.01(84.18)	•loss of organic part of the complex and formation of CuO.
5	[ZnL(H_2O)]$6.5H_2O$	30-125	36.12(36.16)		•loss of $6.5H_2O$ (hydrated), 2 NH_3 and O_2 gases.
		125-260	3.57(3.60)		•loss of H_2O (coordinated).
		260-1300	43.24(43.28)	82.93(83.04)	•loss of organic part of the complex and formation of ZnO.

6.2.9. X-ray diffraction studies

XRD pattern of the Cr(III) complex is shown in Fig. 1. The XRD pattern of the metal complex shows well defined crystalline peaks indicating that the sample was crystalline in phase [22,23]. The metal complexes show sharp crystalline XRD patterns, which differ considerably from that of the ligand. The appearance of crystallinity in the metal–phosphorus Schiff base complex is due to the inherent crystalline nature of the metallic compound. The grain size of the metal–phosphorus Schiff base complexes, d_{XRD} was calculated using Scherre's formula [24] by measuring the full width at half maximum of the XRD peaks.

$d_{XRD} = 0.9\lambda/\beta(Cos\theta)$,

where 'λ' is the wavelength, 'β' is the full width at half maximum and 'θ' is the peak angle. The complex has the average crystallite size of 32 suggesting that the complex is nanocrystalline.

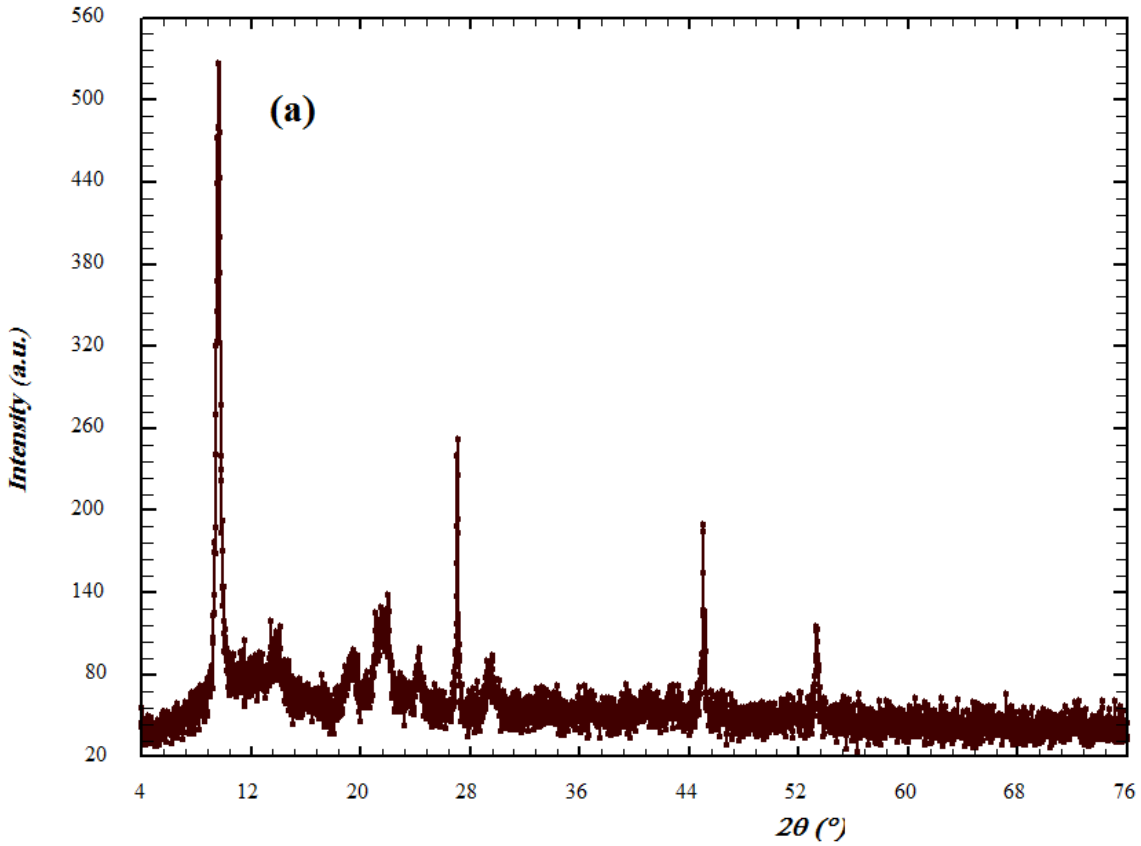

Figure 1. XRD spectrum of Cr(III) complex.

6.2.10. Cyclic voltammetric study

The electrochemical behavior of H_2L and its Co(II), Ni(II) and Cu(II) complexes (Fig. 1) were investigated in MeCN with a scan rate of 100 mV s^{-1}. The cyclic voltammogram of the free ligand displayed three cathodic peaks and one anodic peak. Three well–defined cathodic peaks at about +342 mV, −1186 V and −1698 mV and one anodic peak at about +736 mV were observed. The cathodic peaks were assigned to the reduction of the azomethine group. The copper complexes are redox active and show a cyclic voltammogram response in the potential range 0.8–1.8V assigned to the Cu(II)/Cu(I) couple. The nonequivalent current intensity of cathodic and anodic peaks (ic/ia=0.8 V) indicates a quasi–reversible behavior. It has been shown that the formal redox potential of Cu(II)/Cu(I) couple is dependent on factors such as coordination number, hard/soft nature of the ligands and bulkiness of the ligands. The cobalt complexes exhibit one electron quasi reversible transfer process with a peaks at E_{pa}= 0.8 V, E_{pc}=1.8 V and ΔE_p= 0. 9 V. This gives evidence for quasi reversible Co(II)/Co(I) couple .The cyclic voltammogram of Nickel complexes shows well defined redox process corresponding to the formation of the quasi-reversible Ni(II)/Ni(I) couple. The anodic peak at E_{pa}= 0.7 V and the associated cathodic peak at E_{pc}=1.8 V corresponds to Ni(II)/Ni(I) couple.

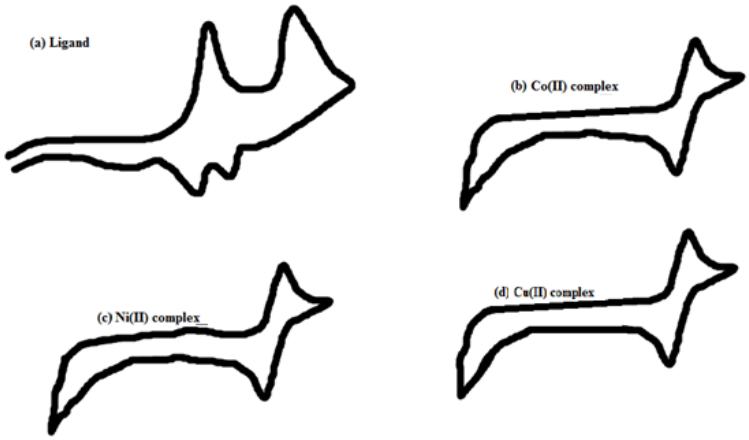

Figure 1. Cyclic voltammograms of (a) Ligand, (b) Co(II), (c) Ni(II) and (d) Cu(II) complexes at 100 mV/s scan rate.

From the above findings, we propose that the coordination occurs through the phosphorus of the phosphorus carbide P–C, carbonyl C=O and the imine NH group to give the structures shown in Scheme 1.

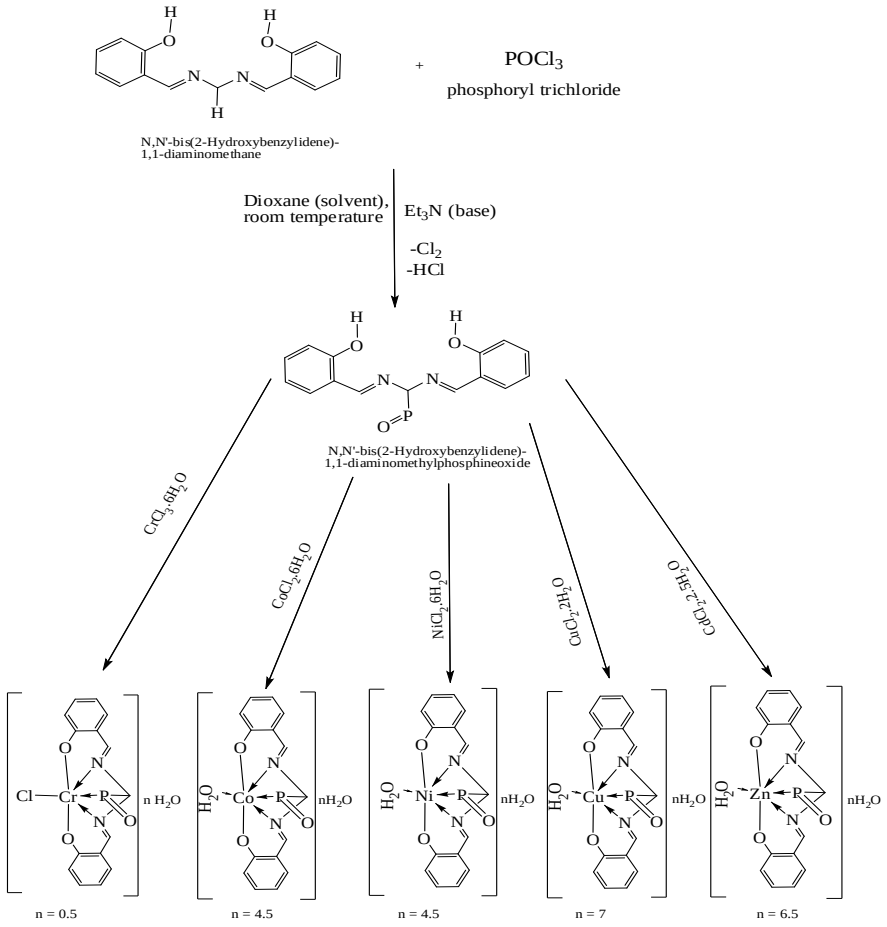

Scheme 1.

References

1. S.S. Kumaravel, S.S. Krishnamurthy, *J. Chem. Soc., Dalton Trans*. 1 (1990) 1119.
2. M.S. Balakrishna, R.M. Abhyankar, J.T. Mague, *J. Chem. Soc., Dalton Trans*. 4 (1990) 1407.
3. M.S. Balakrishna, J.T. Mague, S.M. Mobin, *Inorg. Chem.* 42 (2003) 1272.
4. B. Hoge, C. Thösen, T. Herrmann, P. Panne, I. Pantenburg, *J. Fluor. Chem*. 125 (2004) 831–851.
5. 5. (a) A.M.A. Alaghaz, R.A. Ammar, Eur. J. of Med. Chem. 45 (2010) 1314**;** (b) A.M.A. Alaghaz, *J. Phosphorus, Sulfur, and Silicon, and The Related Elements* 183 (2008)2287. (c) A.M.A. Alaghaz, R.A. Ammar, Al-Azhar Bull. Sci. 21(1) (2010) 233; (d) T. A. Mohamed, I. A. Shabaan, W. M. Zoghaib, J. Husband, R. S. Farag, A. M.A. Alajhaz, *J. of Mol. Struct*. 938 (2009) 263–276.
6. H. Naeimi, K. Rabiei, F. Salimi, *J. Phosphorus, Sulfur, and Silicon, and The Related Elements* 184 (2009)2351.
7. R. Voy, *Chem. Ztg. Chem. Appratus* 21 (1897) 441.
8. U.N. Tripathi, M.S. Ahmed, G. Venubabu, P. Ramakrishna, *J. Coord. Chem*. 60 (2007) 2007.
9. B. Murukan, K. Mohanan, *J. Enzyme Inhib. Med. Chem*. 22 (2007) 65.
10. S. Chandra, A.K. Sharma, *Spectrochim. Acta* A 72 (2009) 851.
11. A. Kumar, P. Sharma, V. K. Gurram and N. Rane, *Bioorg. and Med. Chem. Lett*. 16 (2006) 2484–2491
12. N.M. Youssif, R.Shabana, S.-O.Lawesson,*Bull.Soc.Chem.Fr.* 2 (1986) 383.
13. S. Chandra, Sangeetika, *Spectrochim. Acta* A 60 (2004) 2153.
14. B.N. Figgis, Introduction to Ligand Field Theory. Wiley, New York, 1978; (a) S. Chandra, K. Gupta, Trans. Met. Chem. 27 (2002) 196; (b) S. Chandra, K. Gupta, S. Sharma, *Synth. React. Inorg. Met. Org. Chem.* 31 (2001) 1205; (c) D. Shukla, L. Kumar Gupta, S. Chandra, *Spectrochim. Acta* A 71 (2008) 746.
15. C.K. Jorgensen, *Acta Chim. Scand*. 10 (1956) 500.
16. R.S. Drago, Physical Methods in Chemistry.W.B. Saunders Company,1997, p. 530; (a) F.K. Kneubhul, J. Chem. Phys. 33 (1960) 1074; (b) S. Chandra, L.K. Gupta, *Spectrochim. Acta* 62A (2005) 307.
17. B.J. Hathaway, D.E. Billing, Coord. Chem. Rev. 6 (1970) 143; (a) S. Chandra, L.K. Gupta, *Spectrochim. Acta* 60A (2004) 3079.
18. B.J. Hathaway, J.N. Bradley, R.D. Gillard (Eds.), Essays in Chemistry, Academic Press, New York, 1971, p. 61; (a) S. Chandra, L.K. Gupta, *Spectrochim. Acta* 61A (2005) 269.
19. B.J. Hathaway, R.J. Dudley, P. Nicholls, J. Chem. Soc. A (1968) 1845; (a) S. Chandra, L.K. Gupta, Spectrochim. Acta 60A (2004) 2767.
20. S. Chandra, L.K. Gupta, *Spectrochim. Acta* 60A (2004) 1751; (a) S. Chandra, L.K. Gupta, *Spectrochim. Acta* 60A (2004) 2411.
21. M.W.G. Bolster, The coordination chemistry of aminophosphine oxides and related compounds, Thesis, Leiden, 1972, pp. 88, 89, 95, 98, 100.
22. A.H. Yaacob, Mater. Forum. 29 (2005) 199
23. E.R. Souaya, W.G. Hanna, E. Isamil, N. Milad, *Molecules* 5 (2000) 1121.
24. B.D. Cullity, Elements of X-ray Diffraction, second ed. Addison-Wesley, Publisher, Philippines, 1978.

© 2013 by ESG (www.electrochemsci.org)